PHYSICAL REVIEW B **89**, 035104 (2014)

GW quasiparticle calculations with spin-orbit coupling for the light actinides

Towfiq Ahmed,[1] R. C. Albers,[1] A. V. Balatsky,[1,2,3] C. Friedrich,[4] and Jian-Xin Zhu[1,2,*]
[1]*Theoretical Division, Los Alamos National Laboratory, Los Alamos, New Mexico 87545, USA*
[2]*Center for Integrated Nanotechnologies, Los Alamos National Laboratory, Los Alamos, New Mexico 87545, USA*
[3]*NORDITA, KTH Royal Institute of Technology and Stockholm University, Roslagstullsbacken 23, 106 91 Stockholm, Sweden*
[4]*Peter Grünberg Institut and Institute for Advanced Simulation, Forschungszentrum Jülich and JARA, D-52425 Jülich, Germany*
(Received 16 September 2013; revised manuscript received 6 December 2013; published 6 January 2014)

We report on the importance of *GW* self-energy corrections for the electronic structure of light actinides in the weak-to-intermediate coupling regime. Our study is based on calculations of the band structure and total density of states of Np, U, and Pu using a one-shot *GW* approximation that includes spin-orbit coupling within a full potential LAPW framework. We also present RPA screened effective Coulomb interactions for the f-electron orbitals for different lattice constants, and show that there is an increased contribution from electron-electron correlation in these systems for expanded lattices. We find a significant amount of electronic correlation in these highly localized electronic systems.

DOI: 10.1103/PhysRevB.89.035104 PACS number(s): 71.10.−w, 31.15.A−, 71.15.Qe, 71.27.+a

I. INTRODUCTION

With significantly localized and partially filled f electrons, the light actinide metals have both strong electronic correlation effects and spin-orbit (SO) coupling present in their electronic structure. Many theoretical tools have been developed in the recent years in order to address the strong correlation aspect, which is still considered to be one of the most challenging problems of modern condensed matter physics. For example, many-body treatments of the model Hamiltonian approach, such as Hubbard[1] and periodic Anderson[2] models, have been extensively used to study and explain the electronic structures of the narrow band systems. Particularly for the δ phase of plutonium (Pu), the dynamical mean-field theory (DMFT)[3] provides a theoretical volume in good agreement with the experimental measurement.[4] The δ phase of Pu in particular involves a crossover of itinerant-to-localized behavior in the light actinide series, and has hence been much studied. DMFT has been quite successful in predicting its several electronic features, including the $5f$ occupancy of its valence band.[5–7]

Within the scope of first-principles theory, several developments are currently in progress. The LDA+U method was first proposed by Anisimov *et al.*[8] Although the method relies on the Hubbard U parameter, which is not known exactly, such hybrid methods have been used successfully in accurate description of electronic structure and spectroscopies of many systems such as the transition-metal oxides and high-T_c cuprates.[9–13] Addressing strong correlation in a completely parameter-free manner is often desirable, but requires going beyond the local density approximation (LDA) of conventional density functional theory (DFT). Constrained random phase approximation (cRPA) and constrained LDA (cLDA) are two most popular methods in estimating Hubbard parameters, albeit with limited success.[14,15] Such combinations have been further extended by constructing a quasiparticle *GW* self-energy[16,17] from single or multiband Hubbard model[18] and have been successfully implemented for calculating the spectroscopy of many correlated d- or f-electron systems.[19,20] For the light actinides and Pu, parameter-free *GW* calculations[21] in the absence of SO coupling have shown significant band renormalization effects.

The second essential ingredient for understanding the electronic structure of the actinide elements is their strong SO coupling, which must be incorporated simultaneously with the many-body correlation effects. Within the *GW* approximation, a Dirac-relativistic approach has been implemented in a fully self-consistent manner in order to study Pu and Am metals.[22] In this paper, spin-orbit coupling was implemented within a scalar relativistic framework that uses an LS basis instead of the fully relativistic JJ basis. The LS scheme is particularly convenient for most condensed matter systems.[23] In addition, Hund's rules have a simpler realization in an LS basis when compared to a JJ basis,[23] and it is much easier to treat magnetism when spin and orbital quantum numbers can be clearly identified.

In this paper, we have calculated the LDA and *GW* renormalized band structure of U, Np, Pu, and an extended Pu system. With increasing lattice constants and partially filled f orbitals, these $5f$-electron systems allow us to understand the correlation physics from itinerant to localized behavior for elemental materials, where the SO coupling is comparable to the effective $5f$ band widths. Within the same *GW* approximation, we have also evaluated the average screened Coulomb interaction $W(\omega = 0)$. In the weakly interacting electronic systems, the *GW* self-energy is well known to incorporate the dynamic correlation for both short- and long-ranged Coulomb interactions. By using a standard first-principles method, our calculations provide an important benchmark of the significance of the correlation strength in the light actinides that might further be refined using *GW* as a starting point while also including the effects of SO coupling.

II. FORMALISM

The relativistic extension of the quasiparticle correction is straightforward due to the single-particle nature of spin-orbit (SO) interaction term, which can be simply added to the single-particle Hamiltonian. Because of the coupling between the spin and orbital degrees of freedom, the projected electronic spin $\hat{S}_z$ is no longer a good quantum number. Therefore diagonalization of the Hamiltonian gives Bloch states that are given by a linear combination of both spin up (↑) and down

(↓) states:

$$\psi_{\mathbf{kn}}(\mathbf{r},s) = \psi^{\uparrow}_{\mathbf{kn}}(\mathbf{r})\chi^{\uparrow}(s) + \psi^{\downarrow}_{\mathbf{kn}}(\mathbf{r})\chi^{\downarrow}(s)\,. \tag{1}$$

Here, **k** is the Bloch vector, **s** is the spin degree of freedom, and **n** is the band index.

Accordingly, the single-particle Green's function exhibits off-diagonal elements in spin space (up-down and down-up) enabling spin-flip processes. The relativistic generalization[24,25] of Hedin's GW equations[16,26] thus begins with a spin-dependent formulation of the Green's function:

$$G_{\alpha\beta}(\mathbf{r},\mathbf{r}';\omega) = \sum_{\mathbf{kn}} \frac{\psi^{\alpha}_{\mathbf{kn}}(\mathbf{r})\psi^{\beta *}_{\mathbf{kn}}(\mathbf{r}')}{\omega - \epsilon_{\mathbf{kn}} + i\eta\,\mathrm{sgn}(\epsilon_{\mathbf{kn}} - \epsilon_{\mathbf{F}})}\,, \tag{2}$$

where α and β represent spin up (↑) or down (↓) components, η is a positive infinitesimal, $\epsilon_{\mathbf{kn}}$ is the eigenvalue for diagonalized single-particle Hamiltonian, and ϵ_F is the Fermi energy. Within the random phase approximation (RPA), the polarization function can be obtained as

$$P(\mathbf{r},\mathbf{r}';\omega) = \frac{-i}{2\pi}\sum_{\alpha\beta}\int G_{\alpha\beta}(\mathbf{r},\mathbf{r}';\omega+\omega')G_{\beta\alpha}(\mathbf{r}',\mathbf{r};\omega')\mathbf{d}\omega'. \tag{3}$$

The screened Coulomb interaction $W = V + VPW$ therefore indirectly depends on the SO coupling through the spin-dependent Green's function. Here, V is the bare unscreened Coulomb interaction before the RPA screening, and W is the RPA screened Coulomb interaction, $W(\omega) = \epsilon^{-1}_{\mathbf{RPA}}(\omega)V$. Finally, the spin-dependent matrix elements of the GW self-energy can be constructed following Hedin's prescription as

$$\Sigma_{\alpha\beta}(\mathbf{r},\mathbf{r}';\omega) = \frac{i}{2\pi}\int G_{\alpha\beta}(\mathbf{r},\mathbf{r}';\omega+\omega')W(\mathbf{r},\mathbf{r}';\omega')e^{i\eta\omega'}\mathbf{d}\omega'. \tag{4}$$

A one-shot GW approach is equivalent to the leading order perturbation, and the quasiparticle eigenfunctions are generally approximated as the Bloch functions $\psi^{\uparrow/\downarrow}_{\mathbf{kn}}$. The quasiparticle correction for the eigenvalues is then

$$E_{\mathbf{kn}} = \epsilon_{\mathbf{kn}} + \sum_{\alpha\beta}\left\langle\psi^{\alpha}_{\mathbf{kn}}\middle|\Sigma_{\alpha\beta}(E_{\mathbf{kn}}) - v^{xc}\delta_{\alpha\beta}\middle|\psi^{\beta}_{\mathbf{kn}}\right\rangle. \tag{5}$$

All of the above equations are a spin-dependent generalization for the GW approximation.

To evaluate the effect of lattice spacing and localization of the f orbitals on the correlation strength, we have calculated V_{eff} and U_{eff} as shown in Fig. 4, where V_{eff} and U_{eff} are the average onsite bare and RPA-screened Coulomb interactions of the localized f electrons. These quantities are calculated using the Anisimov prescription[8] by averaging over the orbitals (m_1,m_2,m_3, and m_4) of the angular-momentum-projected bare and screened Coulomb interactions, which are correspondingly defined as $\langle l_1,m_1;l_2,m_2|V|l_3,m_3;l_4,m_4\rangle$ and $\langle l_1,m_1;l_2,m_2|W|l_3,m_3;l_4,m_4\rangle$. To compare with the experimental photoemission spectrum, the spectral function is calculated from the convolution between the density of states (DOS) multiplied by the Fermi function and a Lorentzian function. The purpose of this convolution is to account for the experimental broadening.[27] It is written as

$$A(\omega) = \int_{-\infty}^{\infty}\rho(\omega')\frac{\sigma}{[2\pi(\omega-\omega')]^2 + (\sigma/2)^2}\frac{1}{e^{\omega'/kT}+1}d\omega', \tag{6}$$

where $\rho(\omega)$ is the total DOS, k is the Boltzman constant, T is temperature, at which the experiment was performed, and σ is the experimental broadening.

III. COMPUTATIONAL METHODOLOGY

For most of our calculations, we have used the one-shot relativistic extension[28] of the GW self-energy correction implemented in the code SPEX.[29] In this approach, when the SO coupling is present, the single-particle Green's function is represented in terms of the spin-dependent Bloch band states. The polarization function is then evaluated within the RPA approximation, which determines the screened Coulomb interaction and single-particle self energy. The latter gives the quasiparticle correction. We refer to Ref. 29 for more technical details.

In practice, computational methods are developed by expressing the Bloch states in a suitable basis such as plane waves, linear muffin-tin orbitals or augmented plane waves. On the Kohn-Sham level, the SO coupling term is incorporated in a second-variational step,[30] where the single-particle Hamiltonian including SO coupling is diagonalized in the basis of single-particle states that are eigenfunctions of the Hamiltonian without the SO term. Therefore the SO coupling effect on the quasiparticle correction is naturally included through the Kohn-Sham single-particle states, without the need for an *a posteriori* treatment, see Refs. 31 and 32 for a detailed discussion.

In our calculations, we used a full potential LAPW basis with an SO interaction in the DFT code FLEUR[33] along with a quasiparticle correction in the one-shot GW code, SPEX.[29] Unlike other GW relativistic calculations,[22] instead of an imaginary frequency approach that is analytically continued to real frequencies, our method employs a contour-integration technique in which the self-energy is calculated directly on a real-frequency mesh. This avoids all the well-known sensitivities of the results on the analytic-continuation algorithms,[34] and hence reduces this uncertainty. Our calculations are based on the one-shot GW that involves a single iteration of the GW equations, where the input quantities are the LDA eigenvalues and eigenfunctions. Our self-consistent LDA calculations were converged using $13 \times 13 \times 13$ k points in the Brillouin zone (BZ), and the one-shot GW calculations with 64 k points in the BZ. For metals, a one-shot GW approach has been shown to be in better agreement with experiment than fully self-consistent GW calculations,[35,36] which miss important vertex corrections that are believed to be essential for predicting the correct plasmon energies and for canceling other deficiencies generated in the self-consistent cycle; these defects seem to be absent in the one-shot approach. Hence the standard one-shot calculation may provide a better benchmark than full self-consistency.

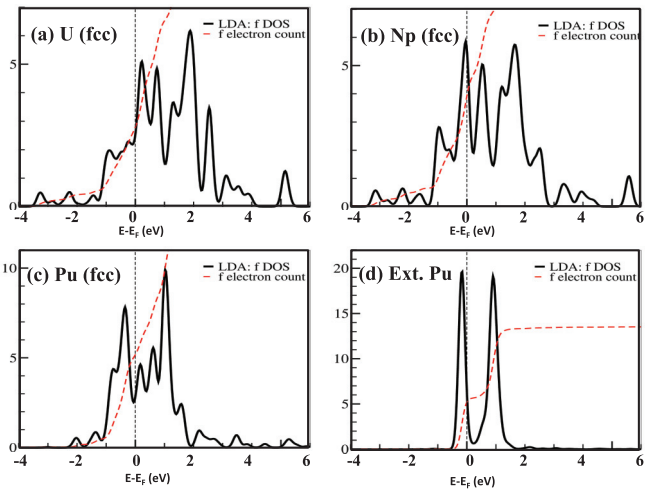

FIG. 1. (Color online) LDA calculated angular momentum projected f-DOS for fcc U, Np, δ-Pu and extended Pu. The vertical dashed line is at the Fermi energy, $E_F = 0$ eV. The dashed curve (red) is the cumulative valence f-electron number (integrated f-DOS). Spin-orbit splitting is most noticeable for the heavier (more localized) actinides.

IV. LATTICE STRUCTURE AND SO COUPLING

Our investigation of electronic correlation from an intermediate to a strong-coupling regime includes three light-actinide elements U, Np, and Pu. This enables us to study variations in the correlation strength simultaneously with a changing SO coupling. Within the phases of the light actinides, a high-temperature fcc δ-Pu phase is by far the most interesting. With a unit cell volume of 168 a_0^3 (with a_0 being the Bohr radius) and a lattice constant of $a_{\mathrm{Pu}} = 4.64$ Å, δ-Pu is known to involve both itinerant and localized electrons, i.e., has a dual-nature f-orbital character.

In order to see clear trends in the physical and electronic properties, we have chosen to do all of our calculations in the same fcc crystal structure as δ-Pu. Other crystal structures would change relative near-neighbor distances and hence would modify the various hybridizations present in the calculations in a way that would modify correlation strength (for an example of how significant these changes would be, see Ref. 6). This problem presents a quandary in that U and Np have no fcc phases. To resolve this issue, we have chosen to do calculations for an fcc crystal structure for U and Np at a volume per atom that is equivalent to the most reasonable high-temperature cubic phase in these elements, which turns out to be bcc in both cases. More precisely, we refer to the γ-U and γ-Np bcc phases with respective unit cell volumes[37] of 138.89 a_0^3 and 129.9 a_0^3. We refer to our fcc calculations as γ-U (fcc) and γ-Np (fcc) to indicate how we have chosen the lattice constant for these calculations, which have the modified lattice constants, $a_{\mathrm{U}} = 4.35$ Å and $a_{\mathrm{Np}} = 4.25$ Å, which are both smaller than a_{Pu} and hence are anticipated to show more itinerant electronic behavior. Finally, we have also considered an fcc-Pu system with an enlarged lattice constant of $a = 6.64$ Å. Such a fictitious system allows us to understand the strong electronic correlation in an extremely localized limit, where the overlap and hybridization between the neighboring $5f$ orbitals is minimal.

TABLE I. Experimental lattice parameters and calculated peak split (Δ) and Coulomb interaction for U, Np, Pu, and extended Pu.

Element	U	Np	Pu	ext-Pu
Z	92	93	94	94
$5f$ valence occ.	3	4	5	5
Original crystal symm.	bcc (γ)	bcc (γ)	fcc (δ)	fcc
Considered symm.	fcc	fcc	fcc	fcc
Unit-cell volume (a.u.)	139.9	129.9	168.0	560.0
FCC lattice constants (Å)	4.35	4.25	4.64	6.64
Δ_{SO} (eV)	0.87	0.95	1.17	1.17
Δ_{LDA} (eV)	1.50	1.69	1.35	1.17
Δ_{GW} (eV)	1.61	1.71	1.91	2.57
$\Delta_{\mathrm{corr}} = \Delta_{GW} - \Delta_{\mathrm{LDA}}$ (eV)	0.11	0.02	0.56	1.4
$\Delta_{\mathrm{Xtal}} = \Delta_{\mathrm{LDA}} - \Delta_{\mathrm{SO}}$ (eV)	0.63	0.74	0.18	0.00
V_{init} (eV)	8.23	4.47	10.21	10.36
W_{screened} (eV)	5.68	2.36	7.74	8.69

Figure 1 shows the LDA calculated angular-momentum-projected f-DOS for all of these cases. For the enlarged Pu lattice constant calculations, as shown in Fig. 1(d), the dominant peak split near Fermi energy is mainly due to SO coupling and is approximately in the atomic limit. In our LDA calculations for U and Np, hybridization, crystal-field, and SO splitting were about the same order of magnitude [see Figs. 1(a) and 1(b)]. With the slightly larger lattice constant in δ-Pu, the larger SO splitting separates the DOS into two peaks, which are mainly $j = 5/2$ for the lower peak and $7/2$ for the upper peak, as shown in Fig. 1(c), whereas the two j components are more mixed for U and Np. Besides SO and crystal fields, which are well captured in DFT, one must also consider the missing long- and short-ranged dynamical correlations, which are the main focus of the remaining sections. For reference, some lattice parameters and calculated SO splitting from the f-DOS are listed in Table I.

V. QP DOS AND BAND RENORMALIZATION

In previous studies using a relativistic self-consistent GW scheme for the actinide elements,[22] the importance of a quasiparticle treatment along with SO coupling was shown to be particularly important for δ-Pu. In another GW calculation without SO coupling by Chantis *et al.*,[21] the band structure of δ-Pu was found to have significant renormalization effect in the presence of crystal fields, indicating that electronic correlation of δ-Pu lies in between the intermediate and strong coupling limit. Here, we systematically investigate correlation in the electronic structure for the four different systems including δ-Pu with different interatomic distances. The real part of the self-energy GW corrections causes a change in the position of the Fermi energy due to the different size of the energy shifts for the more localized f states relative to the other itinerant s-p-d states. To handle this, in our metallic calculations, we determine the Fermi energy according to its definition by requiring that the integrated total DOS below the Fermi energy have the correct number of electrons. We then measure all energies with respect to the Fermi energy ($E_F = 0$).

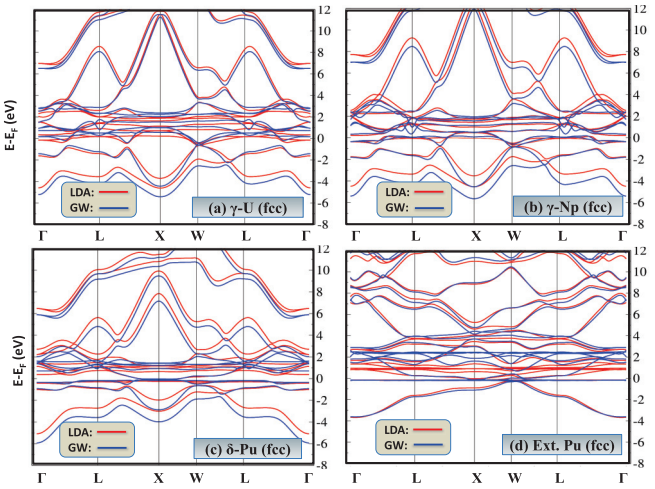

FIG. 2. (Color online) LDA (red) and GW renormalized (blue) band structure of fcc U, Np, Pu, and extended Pu in (a),(b),(c), and (d) accordingly. Bands are calculated along Γ-L-X-W-L-Γ symmetry line and the Fermi energy is set at 0 eV. An fcc crystal structure is used for all calculations.

The bands near the Fermi energy are plotted along Γ-L-X-W-L-Γ high-symmetry line. The GW renormalized bands are plotted in blue lines while the LDA band structures are shown in red lines in Fig. 2; the same color scheme is followed for the total DOS shown in Fig. 3. As expected, fcc Np, which has the smallest lattice spacing $a_{\mathrm{Np}} = 4.25\mathring{A}$, shows the largest dispersion of bands, [see Fig. 2(b)]. On the other hand, the $5f$-electron bands in the extended δ-Pu are the least dispersive. The very localized extended Pu system has very flat bands [see Fig. 2(d)]. In this system, the GW corrections cause a large shift in the unoccupied $j = 7/2$ component of the $5f$ orbitals to higher energy [cf. Fig. 3(d)] due to the nonlocal self-energy operator that acts like an effective Hubbard U in the calculations. In general, the occupied valence electrons

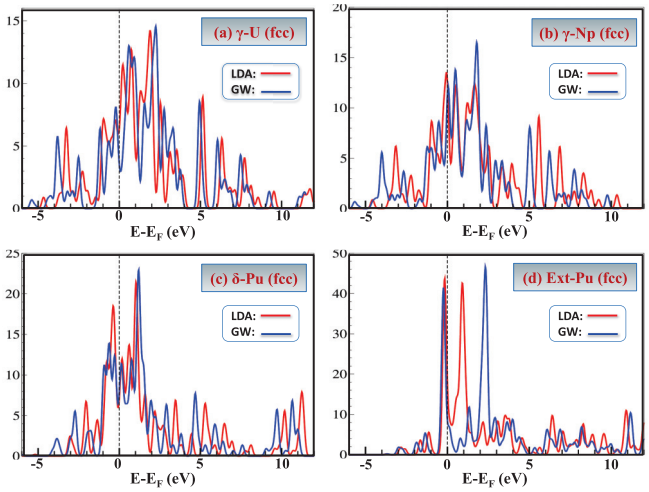

FIG. 3. (Color online) Total density of states corresponding to LDA (red) and GW (blue) band-structure calculations presented in Fig. 2 for (a) U, (b) Np, (c) δ-Pu, and (d) extended Pu. Vertical dashed lines are at the Fermi energy at 0 eV.

can be divided into itinerant states, predominantly $7s^2$ and $6d^1$ (because of their high principal quantum numbers, these have many nodes in the core region for orthogonalization to lower principal quantum number atomic states, which cause a large curvature or high kinetic energy), and localized states, the $5f$ electrons. Similar to GW calculations on uranium,[38] the f states are shifted up relative to the itinerant states (bottom of the valence band).

The quasiparticle total DOS for all four systems are plotted (blue curve) against LDA total DOS (red curve) in Fig. 3. By QP-DOS we mean that we take into account only the shift in the quasiparticle energy due to the real part of the GW self-energy and ignore any lifetime broadening from the imaginary part. Although the QP-DOS is different from the true DOS, it is helpful for identifying the peak locations and the effects of self-energy shifts on them, which would otherwise be smeared out by the lifetime broadening. In Table I, we have calculated Δ_{SO} by using a very large lattice spacing for U, Np, and Pu similar to what is shown in Fig. 1(d). In this case, hybridization is negligible and we are essentially in the atomic limit. For Δ_{LDA} and Δ_{GW}, we calculated the distance between the dominant $5f$ peaks near Fermi energy. Although the SO splitting is not as distinct due to the crystal field effects, comparison between these peaks with and without self-energy correction helps us reveal the contribution from dynamic correlations. Qualitatively, we can attribute Δ_{Xtal} (see Table I) as a measure of crystal field effect relative to SO coupling, and Δ_{corr} as a measure of correlation correction. From Table I, one finds that the material with the smallest lattice constant, Np, has the most itinerant behavior for the valence electrons with prominent crystal field splitting and is least affected by the quasiparticle correction. On the other hand, extended δ-Pu shows the opposite trend. The itinerant behavior is also evident from the presence of several crystal-field splitting in the total DOS for both Np and U [see Figs. 3(a) and 3(b)]. Spin-orbit splitting is more distinct for δ-Pu in Fig. 3(c), and the unoccupied j=7/2 peak at 1.2-eV shifts slightly to higher energy due to the GW correction. Other states that are between 2 and 12 eV shift significantly downward, and thus band narrowing is not only due to the f-like orbitals, but also involves other (e.g., $6d$) electrons. Similar findings have also been reported by other authors.[22] For extended Pu, where the interatomic distance is too large, the self-energy corrections of the highly localized $5f$ electrons cause the SO coupled peak at 1.2 eV to shift 1.5 eV further to the right [see Fig. 3(d)].

VI. PHOTOEMISSION SPECTRA AND DOS

In Fig. 4, we have compared the available experimental data for δ-Pu with our calculated LDA and one-shot GW-based photoemission spectroscopy (PES) with and without the SO coupling. The band narrowing effect for the one-shot GW is evident for calculations without the SO coupling (see dashed blue line against dashed red line). The same effect was also obtained for elemental uranium solid within the quasiparticle GW without the SO coupling.[38] Inclusion of SO coupling does not show similar trend for GW calculations (solid blue) comparing to LDA (solid red). In the vicinity of Fermi energy, the band renormalization with one-shot GW+SO broadens the

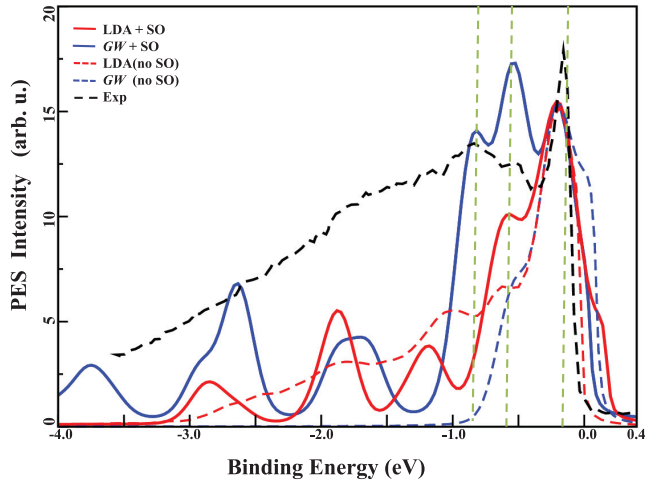

FIG. 4. (Color online) Comparison of experimental photoemission spectrum (dashed black line) of δ-Pu with our calculations using GW+SO (solid blue), LDA+SO (solid red), GW without SO (sashed blue), and LDA without SO (dashed red). Vertical dashed lines show three peaks near E_F on photoemission spectra. Here, $T = 80$ K and $\sigma = 0.2$.

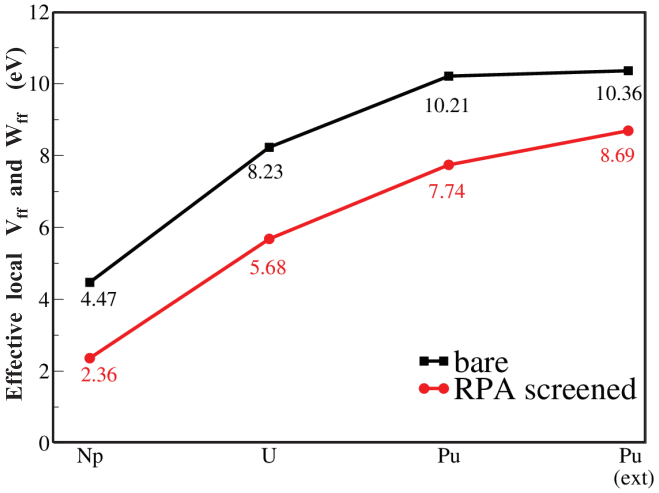

FIG. 6. (Color online) Average (effective) bare (black) and RPA screened (red) Coulomb interaction within occupied $5f$ electrons for Np, U, Pu, and extended Pu. The elements in x axis are ordered according to their increasing lattice spacing. The Coulomb interaction is screened using RPA response function. For more details see the text.

peak. Such results are also consistent with other theoretical calculations.[22] Also, comparing with the experimental PES,[39] the GW+SO calculations (solid blue) are in better agreement with the three peak locations closest to the edge or Fermi energy, which are indicated by vertical dashed lines in Fig. 4. Our real-frequency method for the self-energy is free from the sensitivities[34] caused by an analytical continuation approach. The conservation of occupied valence electrons and spectral weights are also consistent in our method, which can be noticed in Fig. 5 by comparing LDA (solid red) and GW (solid blue) calculations. For the comparison purpose, we have also replotted in the same figure the GW+SO and GW+Dirac calculations as presented in Ref. 22, in which an analytical continuation method is used to obtain the spectral density.

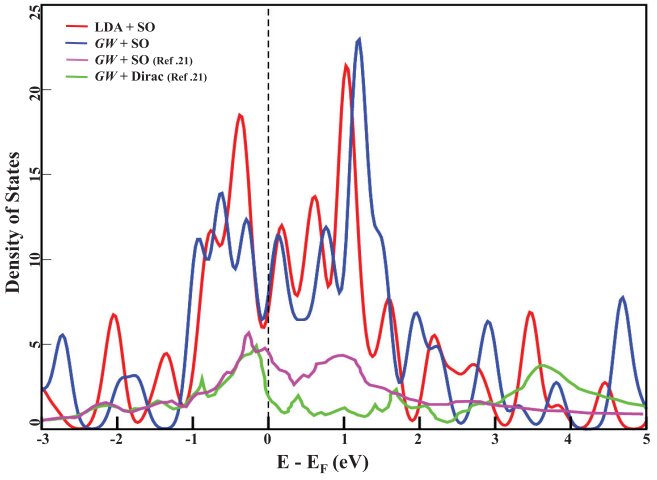

FIG. 5. (Color online) Earlier theoretical calculations of total DOS for δ-Pu using fully relativistic GW (green) and scalar relativistic GW (magenta) method. Our calculations with LDA (solid red) and with one-shot GW + SO approach (solid blue) are also shown.

VII. EFFECTIVE LOCALIZED COULOMB INTERACTION

With increasing lattice spacing, the partially filled f orbitals become more localized and onsite Coulomb interaction becomes stronger. Such situations are most commonly realized as Hubbard-like systems in a model Hamiltonian approach, where $U \gg t$ with U being the Hubbard parameter (e.g., onsite Coulomb interaction), and t the hopping parameter. Within first-principles approach, there have been numerous attempts to determine U from the electronic structure calculation such as the constrained LDA (cLDA) and RPA (cRPA).[14,15] The magnitude of U often provides a good measure for static electronic correlation and is used as an input parameter for LDA+U or LDA+DMFT calculations. Because our GW calculations automatically include a screened Coulomb interaction $W(\omega)$ evaluated within an RPA response function, it is useful to provide these results as another way to show a predicted correlation strength for the different actinides. Projecting W on f orbitals at $\omega = 0$, in Fig. 6, we present the calculated local screened interaction $W_{ff}(\omega = 0)$. In addition, we also show the projected bare Coulomb interaction V_{ff} for comparison. The elements are ordered according to their lattice constant along x axis. We observe that the screened Coulomb interaction scales with the bare one, both increasing with enlarged lattice spacing.

VIII. CONCLUSION

We have reported our findings on the electronic correlations in light actinide systems using the one-shot GW approximation with spin-orbit coupling included. By systematically

tuning from itinerant to localized regime in a set of $5f$ systems, our calculations have shown the effectiveness of relativistic GW correction in describing the correct behavior of electronic structure in the intermediate coupling regime. Thus our calculations provide an important benchmark on the way to a complete description of the electronic structure of light actinides that might be further refined within the GW+DMFT[40] like methods using GW as a starting point.

ACKNOWLEDGMENT

We thank A. Svane, N. E. Christensen, M. van Schilfgaarde, and A. N. Chantis for useful discussions and collaboration on related work. This work was supported by U.S. DOE at LANL under Contract No. DE-AC52-06NA25396, the LANL LDRD Program (T.A., R.C.A. & J.-X.Z.), and the Europe VR Program (A.V.B.).

*Author to whom correspondence should be addressed: jxzhu@lanl.gov; http://theory.lanl.gov

[1] J. Hubbard, Proc. R. Soc. London A **276**, 238 (1963).
[2] P. W. Anderson, Phys. Rev. **124**, 41 (1961).
[3] S. Y. Savrasov, G. Kotliar, and E. Abrahams, Nature (London) **410**, 793 (2001).
[4] N. Cooper, Los Alamos Sci. **26** (2000).
[5] J.-X. Zhu, A. K. McMahan, M. D. Jones, T. Durakiewicz, J. J. Joyce, J. M. Wills, and R. C. Albers, Phys. Rev. B **76**, 245118 (2007).
[6] A. Svane, R. C. Albers, N. E. Christensen, M. van Schilfgaarde, A. N. Chantis, and J.-X. Zhu, Phys. Rev. B **87**, 045109 (2013).
[7] J.-X. Zhu, P. H. Tobash, E. D. Bauer, F. Ronning, B. L. Scott, K. Haule, G. Kotliar, R. C. Albers, and J. M. Wills, Europhys. Lett. **97**, 57001 (2012).
[8] V. I. Anisimov, F. Aryasetiawan, and A. I. Lichtenstein, J. Phys.: Condens. Matter **9**, 767 (1997).
[9] T. Ahmed, J. J. Kas, and J. J. Rehr, Phys. Rev. B **85**, 165123 (2012).
[10] H. Jiang, R. I. Gomez-Abal, P. Rinke, and M. Scheffler, Phys. Rev. Lett. **102**, 126403 (2009).
[11] M. Cococcioni and S. de Gironcoli, Phys. Rev. B **71**, 035105 (2005).
[12] V. I. Anisimov, I. V. Solovyev, M. A. Korotin, M. T. Czyżyk, and G. A. Sawatzky, Phys. Rev. B **48**, 16929 (1993).
[13] K. Nakamura, R. Arita, Y. Yoshimoto, and S. Tsuneyuki, Phys. Rev. B **74**, 235113 (2006).
[14] F. Aryasetiawan, M. Imada, A. Georges, G. Kotliar, S. Biermann, and A. I. Lichtenstein, Phys. Rev. B **70**, 195104 (2004).
[15] F. Aryasetiawan, K. Karlsson, O. Jepsen, and U. Schönberger, Phys. Rev. B **74**, 125106 (2006).
[16] L. Hedin and S. Lundqvist, in *Solid State Physics* edited by F. Seitz, D. Turnbull, and H. Ehrenreich, Vol. 23 (Academic Press, New York, 1969), pp. 1–81.
[17] L. Hedin, Phys. Rev. **139**, A796 (1965).
[18] T. Das, R. S. Markiewicz, and A.Bansil, Phys. Rev. B **81**, 174504 (2010).
[19] T. Ahmed, T. Das, J. J. Kas, H. Lin, B. Barbiellini, F. D. Vila, R. S. Markiewicz, A. Bansil, and J. J. Rehr, Phys. Rev. B **83**, 115117 (2011).
[20] S. Basak, T. Das, H. Lin, J. Nieminen, M. Lindroos, R. S. Markiewicz, and A. Bansil, Phys. Rev. B **80**, 214520 (2009).
[21] A. Chantis, R. Albers, A. Svane, and N. Christensen, Philos. Mag. **89**, 1801 (2009).
[22] A. Kutepov, K. Haule, S. Y. Savrasov, and G. Kotliar, Phys. Rev. B **85**, 155129 (2012).
[23] R. D. Cowan, *The Theory of Atomic Structure and Spectra* (University of California Press, Berkeley, 1981).
[24] F. Aryasetiawan and S. Biermann, Phys. Rev. Lett. **100**, 116402 (2008).
[25] F. Aryasetiawan and S. Biermann, J. Phys.: Condens. Matter **21**, 064232 (2009).
[26] L. Hedin, Physica B **158**, 344 (1989).
[27] A. O. Shorikov, A. V. Lukoyanov, M. A. Korotin, and V. I. Anisimov, Phys. Rev. B **72**, 024458 (2005).
[28] R. Sakuma, C. Friedrich, T. Miyake, S. Blügel, and F. Aryasetiawan, Phys. Rev. B **84**, 085144 (2011).
[29] C. Friedrich, S. Blügel, and A. Schindlmayr, Phys. Rev. B **81**, 125102 (2010).
[30] C. Li, A. J. Freeman, H. J. F. Jansen, and C. L. Fu, Phys. Rev. B **42**, 5433 (1990).
[31] I. Aguilera, C. Friedrich, G. Bihlmayer, and S. Blügel, Phys. Rev. B **88**, 045206 (2013).
[32] I. Aguilera, C. Friedrich, and S. Blügel, Phys. Rev. B **88**, 165136 (2013).
[33] http://www.flapw.de.
[34] O. Gunnarsson, M. W. Haverkort, and G. Sangiovanni, Phys. Rev. B **81**, 155107 (2010).
[35] F. Aryasetiawan and O. Gunnarsson, Rep. Prog. Phys. **61**, 237 (1998).
[36] W. G. Aulbur, L. Jönsson, and J. W. Wilkins, in *Solid State Physics*, edited by H. Ehrenreich and F. Spaepen (Academic, New York, 2000), pp. 1–218.
[37] M. D. Jones, J. C. Boettger, R. C. Albers, and D. J. Singh, Phys. Rev. B **61**, 4644 (2000).
[38] A. N. Chantis, R. C. Albers, M. D. Jones, M. van Schilfgaarde, and T. Kotani, Phys. Rev. B **78**, 081101(R) (2008).
[39] A. J. Arko, J. J. Joyce, L. Morales, J. Wills, J. Lashley, F. Wastin, and J. Rebizant, Phys. Rev. B **62**, 1773 (2000).
[40] S. Biermann, F. Aryasetiawan, and A. Georges, Phys. Rev. Lett. **90**, 086402 (2003).